

# Turbulent Boundary-Layer Control by Means of Spanwise-Wall Oscillation

Kwing-So Choi,\* Jean-Robert DeBisschop,† and Brian R. Clayton‡  
University of Nottingham, Nottingham NG7 2RD, England, United Kingdom

An investigation into the changes in the turbulent boundary-layer structure with a spanwise-wall oscillation was carried out in a wind tunnel using hot-wire anemometry and flow visualization. The main purpose of this study is to experimentally confirm the results of recent direct numerical simulations suggesting that the turbulent skin-friction drag can be reduced by a wall oscillation. The present results clearly indicate that the logarithmic velocity profiles are shifted upward and turbulence intensities reduced by the spanwise-wall oscillation. When the wall oscillation was optimized with a nondimensional wall speed, skin-friction reductions of as much as 45% were observed within five boundary-layer thicknesses downstream of the start of wall oscillation. The mechanism of drag reduction seems to strongly relate to the spanwise vorticity generated by the periodic Stokes layer over the oscillating wall, which affects the boundary-layer profile by reducing the mean velocity gradient within the viscous sublayer. The longitudinal vortices in the near-wall region are also realigned into the spanwise direction, reducing the intensity of streamwise vorticity fluctuations across the boundary layer.

## Nomenclature

$C_f$	= skin-friction coefficient
$C_{f0}$	= skin-friction coefficient without wall oscillation
$H$	= boundary-layer shape factor
$h$	= channel half-height
$Q_x$	= channel flow rate
$R(z)$	= cross-correlation coefficient
$R_\theta$	= Reynolds number based on momentum thickness
$T^+$	= nondimensional time, $Tu^*/\nu$
$T$	= time
$U_\infty$	= freestream velocity
$u^*$	= friction velocity
$u'$	= rms velocity fluctuation
$x, y, z$	= streamwise, normal, and spanwise distance
$x^+$	= nondimensional distance, $xu^*/\nu$
$y^+$	= nondimensional distance, $yu^*/\nu$
$z^+$	= nondimensional distance, $zu^*/\nu$
$\Delta u$	= velocity reduction
$\Delta z$	= amplitude of wall oscillation
$\delta$	= boundary-layer thickness
$\nu$	= kinematic viscosity of the fluid
$\Omega$	= vorticity vector
$\Omega_z$	= spanwise vorticity
$\omega$	= angular velocity of wall oscillation

## Introduction

**T**URBULENCE management is a field in fluid mechanics where the effects of flow manipulation on the turbulence characteristics are studied to improve the efficiency of thermofluid systems. This includes the techniques for reducing drag and surface-flow noise as well as enhancing heat transfer and flow mixing.<sup>1-5</sup> Most of the methods in turbulence management utilize, either explicitly or implicitly, the coherent structure of turbulent shear flows.<sup>6-9</sup> In particular, the importance of the burst events in the boundary layers

has been appreciated by many researchers, who tried to modify the turbulence structure to obtain drag reductions.<sup>10-13</sup> Riblets<sup>14-18</sup> and large eddy break-up devices<sup>19,20</sup> are some of the passive devices extensively studied and known to give skin-friction and surface-flow noise reductions. In essence, these devices modify the structure of turbulent boundary layers by disturbing the sequence of turbulence activities in such a way to reduce the burst events leading to the reduction in energy production. It is also known that the turbulent skin-friction and surface-flow noise can be reduced when the intensity and frequency of the burst events are reduced.

Jung et al.<sup>21</sup> conducted a direct numerical simulation (DNS) study of turbulent channel flow where one of the channel walls was oscillated in a spanwise direction. The domain of their calculation was 1010 wall units in the  $x$  axis, 400 wall units in the  $y$  axis, and 1010 wall units in the  $z$  axis. The mesh size of  $64 \times 129 \times 128$  was used to be able to resolve all of the essential sizes of turbulence eddies within the computational domain, where a fully developed turbulent flow with the Reynolds number of  $3 \times 10^3$  (based on the half-height of the channel and the bulk velocity) was established before the start of wall oscillation. Their result indicates that a 40% reduction in turbulent skin-friction drag can be obtained by a spanwise-wall oscillation only after five periods when the nondimensional period of oscillation  $T^+$  was set to 100. The logarithmic velocity profile of the boundary layer is shifted upward, suggesting that the viscous sublayer is thickened as a result of the spanwise-wall oscillation. It is also shown that there are reductions in the intensities of velocity fluctuations by up to 30%. The basic findings of this investigation were later confirmed by Baron and Quadrio,<sup>22</sup> although their DNS study was limited to the optimum oscillating frequency.

Recently, Laadhari et al.<sup>23</sup> carried out an experimental study to look at the problem at a larger Reynolds number of  $9.4 \times 10^3$  (based on the boundary-layer thickness), showing that the mean velocity gradient of the boundary layer is reduced near the oscillating wall. They also demonstrated that there are reductions in turbulence intensities, suggesting that the skin-friction drag of the turbulent boundary layer may be reduced by the spanwise-wall oscillation. However, no direct measurements of skin-friction coefficient were conducted in this study to confirm the drag reductions observed in the numerical simulations.

Choi<sup>13</sup> discussed several drag reduction strategies for turbulent boundary layers, where a possible mechanism of turbulent drag reduction by the spanwise-wall oscillation is suggested. He argued that the sequence of turbulence events will be disturbed if the wall moves quickly by more than the spanwise correlation distance of near-wall turbulence structure, approximately 50 wall units,<sup>15</sup> leading to a reduction in the energy production of the boundary layer. In other words, the spatial coherence between the longitudinal vortices

Presented as Paper 97-1795 at the AIAA 28th Fluid Dynamics Conference, Snowmass Village, CO, June 29–July 2, 1997; received July 5, 1997; revision received March 12, 1998; accepted for publication March 15, 1998. Copyright © 1998 by the American Institute of Aeronautics and Astronautics, Inc. All rights reserved.

\*Senior Lecturer, Department of Mechanical Engineering. Senior Member AIAA.

†Postdoctoral Research Assistant, Department of Mechanical Engineering; currently Project Analyst, Space Projects Group, Dowty Aerospace, Wolverhampton WV9 5EW, England, United Kingdom.

‡Professor, Department of Mechanical Engineering.

and low-speed streaks may be disrupted, as Baron and Quadrio<sup>22</sup> postulated, by oscillating a wall in a spanwise direction. In practice, the speed of wall oscillation is limited by the type of oscillating mechanism, implying that the frequency of oscillation and its amplitude are important in obtaining maximum drag reductions using this technique.

Active control of drag reduction requires an energy input into the system, and the technique being described here is no exception. In other words, the net energy saving from the spanwise-wall oscillation, if it can be realized, will be the total drag reduction observed less the energy required to activate the system. The effect of wall-oscillation amplitude on the total energy balance was investigated by Baron and Quadrio<sup>22</sup> in their DNS study. Although no net savings were found when the amplitude of the wall oscillation was greater than  $3Q_x/8h$ , net energy savings were obtained at smaller amplitudes. Indeed, there was up to 10% of net energy saving at the wall-oscillation amplitude of  $Q_x/8h$ . This study was carried out at a fixed nondimensional period of  $T^+ = 100$ ; therefore it is expected that there may be a scope of further net energy savings.

It must be emphasized here that the DNS study by Jung et al.<sup>21</sup> was carried out with an oscillating crossflow between the stationary walls, except for a case where one of the channel walls was oscillated in a spanwise direction. On the other hand, all of the numerical simulations by Baron and Quadrio<sup>22</sup> were conducted in a planar channel with a wall oscillated in a spanwise direction. The present experimental study and the investigation of Laadhari et al.<sup>23</sup> were conducted in a wind tunnel by oscillating a boundary-layer wall in a spanwise direction.

The main purpose of the present investigation is to experimentally confirm the results of recent DNS studies, particularly the amount of turbulent drag reduction by a spanwise-wall oscillation. This was conducted by measuring the streamwise development of the skin-friction coefficient over the oscillating wall surface, which has not been carried out in the previous studies. Higher-moment turbulence statistics were also documented and were compared with those of the numerical studies. We are interested in understanding the mechanism of turbulent drag reduction by spanwise-wall oscillation, where an extensive study of the modified structure in the near-wall region of the boundary layer was carried out using the hot-wire anemometry and a flow visualization technique in the present experiment. Finally, an investigation into key parameters of spanwise-wall oscillation was conducted in an effort to optimize this active technique of turbulent drag reduction.

## Experiments

The present experiments were performed in an open-return, low-speed wind tunnel at the University of Nottingham with a  $300 \times 534$  mm working section that was 3.0 m long. The boundary layer was tripped at the inlet of the working section to ensure a fully developed turbulent boundary layer over the test surface. The pressure gradient along the length of the working section was nearly zero. The leading edge of the 500-mm-long oscillating plate was located 2 m downstream of the trip, set flush to the surrounding surface. The sinusoidal oscillation was produced by a crankshaft system, with oscillation frequencies up to 7 Hz and peak-to-peak amplitudes of up to 70 mm. The drive system had a flywheel and a set of counterbalances to maintain a constant angular velocity with minimum vibrations during the experiments. Tests were performed with a freestream velocity  $U_\infty$  between 1.0 and 2.5 m/s with a turbulence intensity of about 0.3%. At the trailing edge of the oscillating plate, the boundary layer without wall oscillation had the following properties:  $\delta = 60$  mm,  $R_\theta = 1.19 \times 10^3$ , and  $H = 1.44$  at  $U_\infty = 2.5$  m/s.

Velocity measurements were made with a Dantec 56C CTA system using a single, miniature, hot-wire probe (Dantec 55P15) having a  $5\text{-}\mu\text{m}$ -diam sensing element that was 1.2 mm long. The hot wire was operated at a constant-temperature mode with an overheat ratio of 1.8, and the data from the anemometer system were sampled at a rate of 2 kHz through an IOTech ADC 488/8S analog-to-digital converter. The probe was mounted on a three-directional traverse gear with  $1.25\text{-}\mu\text{m}$  positioning accuracy through a Digiplan step-motor controller. The bulk of the measurements were made at 10 mm downstream of the trailing edge of the oscillating plate, equivalent to  $x^+ \approx 70$  at  $U_\infty = 2.5$  m/s. Wall-shear stress was determined by

means of the near-wall slope of the mean velocity profile and by use of the Preston tube connected to a differential pressure transducer (Furness Control FC0510) of 0.001-Pa resolution with an accuracy of 0.25% of reading.

Flow visualization of the near-wall turbulence was performed at a freestream velocity of 1.5 m/s using a smoke-wire technique.<sup>15</sup> A pulsed copper-vapor laser with a power output of 15 W at a pulse rate of 10 kHz was used as a light source, which was fanned out with a cylindrical lens to produce a light sheet at 7.5 wall units from the wall. Still photographs with the smoke wire placed at  $y^+ = 4$  were taken using a Nikon F-801 camera with a simultaneous video recording by a Sony CCD-V800E Hi8-color camcorder. A high-speed video recording was also made with a Kodak Ektapro Motion Analyzer, with a shutter speed of  $\frac{1}{500}$  s at 500 fps. Visualization of wall-surface temperature to investigate the behavior of low-speed (high-temperature) streaks was carried out using infrared thermography in real time (25 fps) by uniformly heating a section of the wall surface immediately downstream of the oscillating wall by approximately  $10^\circ\text{C}$ . The Agema 880 infrared thermography system, which is capable of recording images up to 25 fps with a resolution of  $0.07^\circ\text{C}$ , was used in the present investigation. The frequency response of the heated surface was up to 10 Hz owing to the use of a  $25\text{-}\mu\text{m}$ -thick polyethylene terephthalate film spattered with stainless steel, which was isolated from the test surface by a 1.6-mm-thick air cavity.

## Results and Discussion

The mean-velocity profiles obtained from the present study are shown in Fig. 1 in a log-law plot, where all of the profiles were nondimensionalized using the friction velocity for each experimental condition. The curves drawn through the data<sup>24</sup> cover the viscous sublayer, buffer layer, and log-law region, which seem to fit all of the data including those with spanwise-wall oscillation with an amplitude of up to 70 mm ( $z^+ = 490$ ). The logarithmic velocity profiles are seen to collapse onto a single curve in the region of the viscous sublayer but are otherwise shifted upward with an increase in oscillation frequency, suggesting that the skin-friction drag is reduced by the spanwise-wall oscillation. When the outer-scaled velocity profiles are plotted in linear coordinates (Fig. 2), it is clear that the mean-velocity gradient in the near-wall region is significantly reduced with the wall oscillation. This reduction in the mean-velocity gradient, which is also seen in the experimental results of Laadhari et al.,<sup>23</sup> clearly demonstrates that the wall-shear stress of the turbulent boundary layer is reduced by the spanwise-wall oscillation. The inner-scaled velocity profiles given in Fig. 3, on the other hand, show that the extent of the linear region of the viscous sublayer is increased to  $y^+ \approx 10$  or perhaps further at the maximum oscillation frequency (7 Hz) of the present experiment. This is in sharp contrast with the velocity profile without wall oscillation, where the linear velocity region of the viscous sublayer extends only to about  $y^+ = 2.5$ , which is in good agreement with the laser Doppler anemometry measurements by Durst et al.<sup>25</sup>

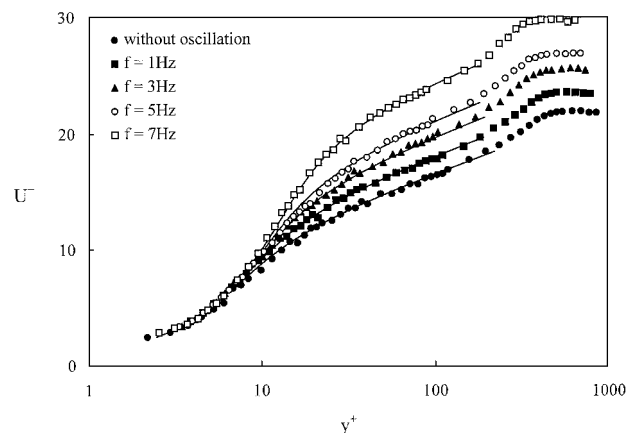


Fig. 1 Logarithmic velocity profiles of the boundary layer 10 mm downstream of the trailing edge of the oscillating plate for different frequencies of wall oscillation ( $\Delta z = 70$  mm).

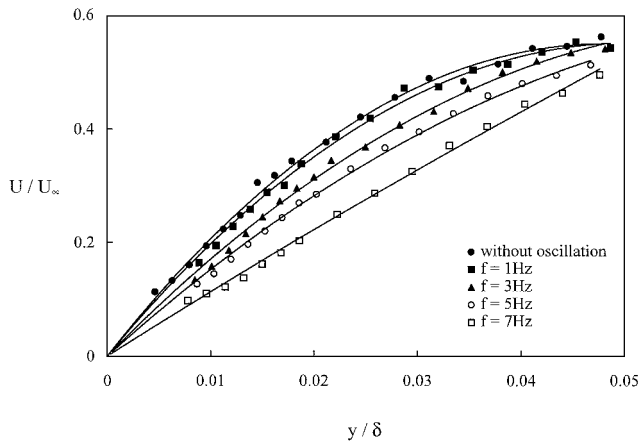


Fig. 2 Outer-scaled velocity profiles in the near-wall region of the boundary layer 10 mm downstream from the trailing edge of the oscillating plate for different frequencies of wall oscillation ( $\Delta z = 70$  mm).

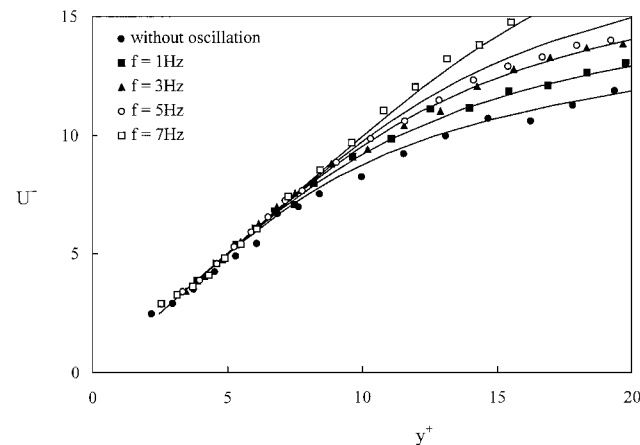


Fig. 3 Inner-scaled velocity profiles in the near-wall region of the boundary layer 10 mm downstream from the trailing edge of the oscillating plate for different frequencies of wall oscillation ( $\Delta z = 70$  mm).

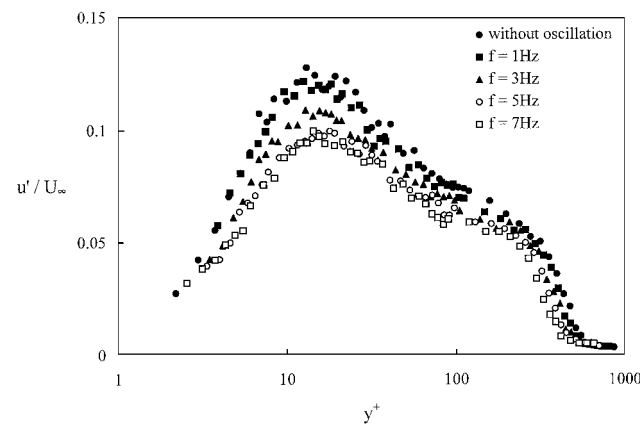


Fig. 4 Turbulent intensity profiles of the boundary layer 10 mm downstream from the trailing edge of the oscillating plate for different frequencies of wall oscillation ( $\Delta z = 70$  mm).

The turbulence intensities of the boundary layer are plotted in Fig. 4 against the nondimensional distance  $y^+$  from the wall, where large reductions in the intensity values are evident within the inner region when the wall is oscillated in a spanwise direction. It seems, however, that the structure of the boundary layer in the outer region is unaltered by the presence of the oscillating wall because the turbulence intensities remain unchanged there. There is a shift in the intensity profiles toward smaller  $y^+$  values (to the left in Fig. 4) due to the reduction in the boundary-layer thickness by the spanwise-wall oscillation. The experimental results of Laadhari et al.,<sup>23</sup> as

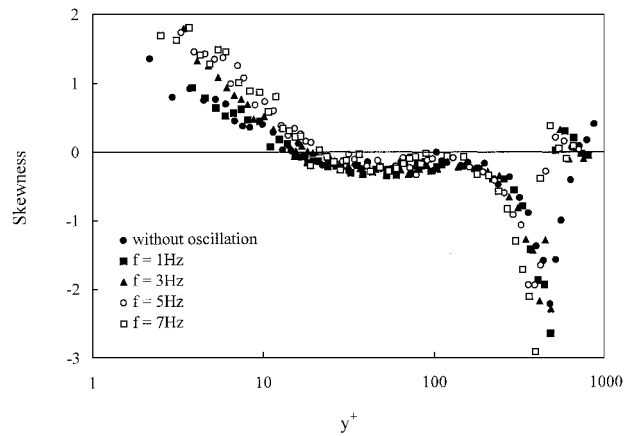


Fig. 5 Skewness profile of the boundary layer 10 mm downstream from the trailing edge of the oscillating plate for different frequencies of wall oscillation ( $\Delta z = 70$  mm).

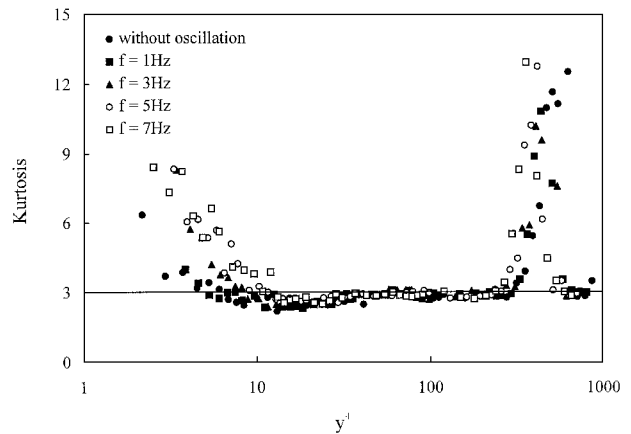


Fig. 6 Kurtosis profile of the boundary layer 10 mm downstream from the trailing edge of the oscillating plate for different frequencies of wall oscillation ( $\Delta z = 70$  mm).

well as numerical data of Jung et al.<sup>21</sup> and Baron and Quadrio,<sup>22</sup> exhibit a similar behavior.

The distribution of skewness and kurtosis of the velocity fluctuations are presented in Figs. 5 and 6, respectively. Both of the higher moments of turbulence statistics seem to be increased within the near-wall region, agreeing very well with the DNS results of Baron and Quadrio.<sup>22</sup> These increases in higher moments can also be interpreted as a manifestation of the increases in viscous sublayer thickness by the spanwise-wall oscillation that have been observed in several drag-reducing flows. Pal et al.<sup>26</sup> were able to demonstrate a strong correlation between the increases in the higher moments of shear stress signal and the amount of turbulent drag reduction with polymer and microbubbles injected into the boundary layer. A similar observation was made by Choi<sup>15</sup> for the turbulent boundary layer over drag-reducing riblets. The reduction in the boundary-layer thickness by the spanwise-wall oscillation is also seen in these figures.

The streamwise variation of skin-friction coefficient  $C_f$  of the boundary layer with spanwise-wall oscillation is shown in Fig. 7. The skin-friction coefficient over the oscillating wall begins to reduce just upstream (about two boundary-layer thicknesses) of the leading edge to reach a maximum level of drag reduction somewhere near the middle of the plate. The present data clearly indicate that there are as much as 45% reductions in the skin-friction coefficient compared with that without wall oscillation, which is in close agreement with the results of DNSs.<sup>21,22</sup> The skin-friction coefficient then seems to revert back gradually toward the level  $C_f/C_{f0} = 1$  corresponding to the condition without wall oscillations in the downstream of the oscillating plate. Nearly 20% reduction in  $C_f$  is still evident after more than two boundary-layer thicknesses from the trailing edge of the oscillating plate.

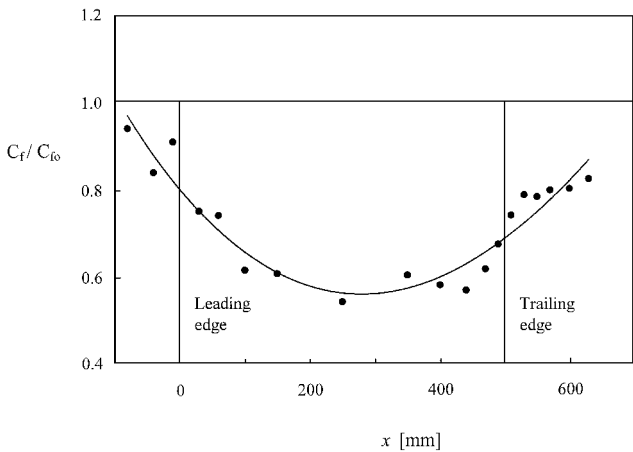


Fig. 7 Downstream variation of skin-friction coefficient  $C_f$  with a spanwise-wall oscillation ( $f = 5$  Hz and  $\Delta z = 50$  mm) as a ratio to the skin-friction coefficient  $C_{f0}$  without oscillation. The leading edge of the 500-mm-long oscillating plate is located at  $x = 0$ .

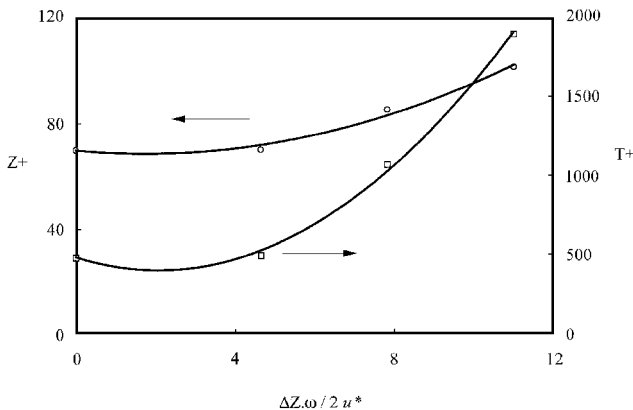


Fig. 8 Effects of spanwise-wall oscillation on the spanwise spacing and the duration of the low-speed streaks, based on the infrared imaging of surface temperature profiles at different wall speeds of spanwise oscillation ( $\Delta z = 50$  mm).

Figure 7 seems to suggest that there is only a narrow plateau in the streamwise variation of  $C_f$  in the present experiment, which leaves a doubt whether the plateau corresponds to a maximum attainable level of drag reduction by a spanwise-wall oscillation. Assuming that the convection velocity of the boundary layer in the near-wall region is about one-third of the freestream velocity, the timescale for the turbulent structure to evolve from the leading edge of the oscillating plate to the location of the observed plateau ( $x = 0.25$  m) is estimated as  $T^+ = 170$ . This is much shorter than was required (about  $T^+ = 500$ ) to reach the maximum level of drag reduction in the DNS results carried out by Jung et al.<sup>21</sup> Therefore, the narrow plateau in the  $C_f$  variation (Fig. 7) may have resulted from a short oscillating plate used in the present experiment, which may not be long enough for the turbulence structure to reach a new equilibrium state with the spanwise-wall oscillation. It is possible, therefore, that a greater drag reduction may be achieved with a longer oscillating plate.

The infrared images of low-speed (high-temperature) streaks of the boundary layer over a uniformly heated section of wall surface were recorded at 10 mm downstream ( $x^+ = 70$ ) from the trailing edge of the oscillating plate. Here, the vertical scan of the infrared camera was disabled, allowing the line images to be recorded in time series at a high scanning frequency of 12.5 kHz. It was observed from the recorded infrared images that several streaks coalesce into a single streak as the wall oscillates, leading to an increase in the streak spacing by the wall oscillation. It also appeared that the meandering motion of the streaks is greatly reduced when the wall is oscillated.

A detailed analysis of these images is summarized in Fig. 8, which shows that the spanwise spacing of the low-speed (high-temperature) streaks and their duration have been increased with an increase in the nondimensional wall speed of spanwise oscillation.

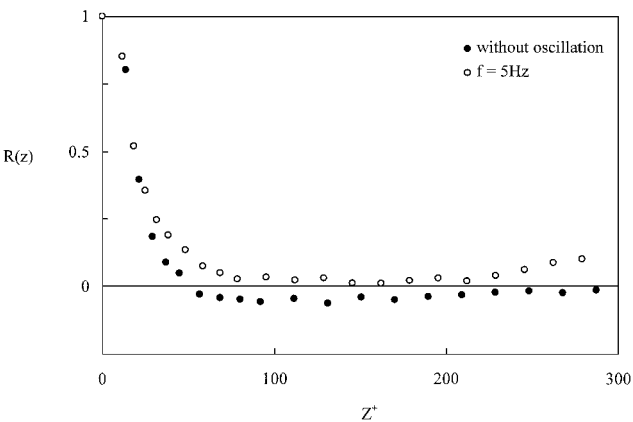


Fig. 9 Effects of spanwise-wall oscillation on the velocity cross-correlation coefficient  $R(z)$  at  $y^+ \approx 0.5$ :  $\circ$ , with wall oscillation ( $f = 5$  Hz and  $\Delta z = 50$  mm), and  $\bullet$ , without wall oscillation.

Indeed, the nondimensional streak spacing  $z^+$  is increased by nearly 45%, whereas the duration of the streaks  $T^+$  is multiplied by a factor of 4 when the wall is oscillated at the near-optimum condition. The results of cross-correlation measurements using hot-wire probes placed close to the wall at  $y^+ = 0.5$  (Fig. 9) seem to support this result. It shows that the velocity cross correlation of the turbulent boundary layer, measured by the distance between the origin and the first zero-crossing point of the cross-correlation coefficient, is increased by about 80% by the spanwise-wall oscillation. Figure 8 suggests, however, that the saturation point for drag reduction does not seem to have been reached yet even at the maximum wall speed of the present study.

When a flat plate is oscillated tangentially in still fluid, a thin layer of periodic shear flow is formed near the wall as a result of viscous diffusion from its surface. This is the well-known Stokes second problem, and the Stokes layer over the oscillating wall is a constant source of vorticity of alternate signs as the wall moves back and forth.<sup>27</sup> If there is a stream of uniform flow over an oscillating wall surface, the vortex sheets produced by the periodic Stokes layer will be convected by the boundary layer exhibiting an oscillatory motion. This can be seen in the flow-visualized pictures Fig. 10a (as the wall moves upward) and Fig. 10b (as the wall moves downward), where the vorticity vector  $\Omega$  is tilted into the spanwise direction, creating a net spanwise component of the vorticity as shown by an arrow in each figure. The numerical study carried out by Baron and Quadrio<sup>22</sup> indeed shows the existence of the local intensity maximum of the spanwise vorticity fluctuations at  $y^+ = 15$ , which can be considered as the location of spanwise vorticity created by the Stokes layer over the oscillating plate.

The effect of a spanwise vorticity on the boundary-layer profile can be examined using a conceptual model presented in Fig. 11. Here, the net spanwise vorticity  $\Omega_z$  created by the periodic Stokes layer over the oscillating wall is located at the edge of the viscous sublayer. From this conceptual model, it can be expected that the mean-velocity gradient in the near-wall region ( $y^+ < 15$ ) will be reduced by the induction of the spanwise vorticity. The mean velocity will be increased outside the viscous sublayer ( $y^+ > 15$ ) on the other hand, shifting the logarithmic velocity profile upward. These behaviors affecting the boundary-layer profiles are clearly seen in the present experimental results in Figs. 2 and 1, respectively. Indeed, the measured changes in the boundary-layer profiles due to wall oscillation (Fig. 12) agree very well with the prediction using the conceptual model (Fig. 11). It is particularly remarkable to note in Fig. 12 that the crossover point of the measured velocity profiles is located at  $y^+ = 25$ , quite consistent with the present conceptual model. It must be emphasized here that the net spanwise vorticity  $\Omega_z$  does not induce any inflection points in the boundary-layer profile as seen in Fig. 3. Therefore, no increases in the level of the burst activity are expected as a result of the generation of the spanwise vorticity over an oscillating wall.

The results of flow visualization in the near-wall region of the boundary layer demonstrate that the pairs of longitudinal vortices

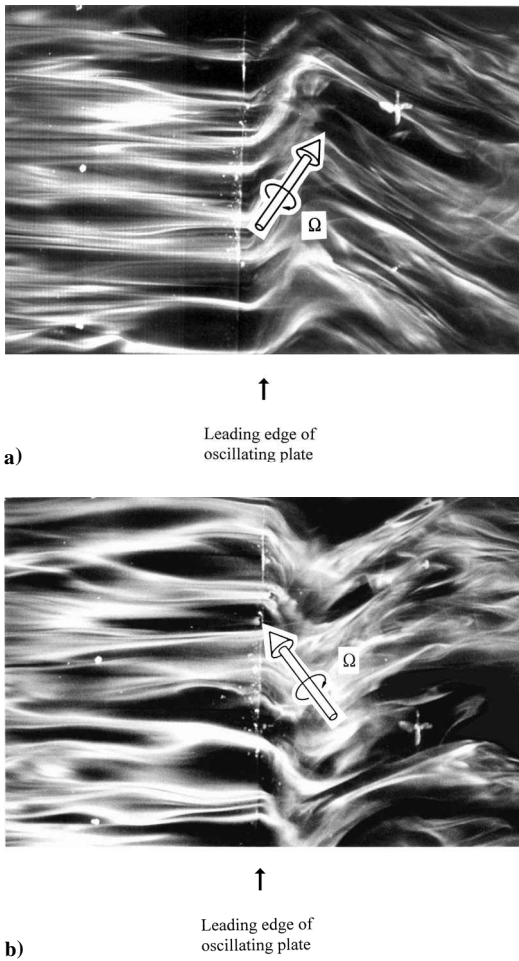


**Fig. 10** Flow visualization of longitudinal vortices in the near-wall region of the boundary layer with a wall oscillation ( $f = 5$  Hz and  $\Delta z = 50$  mm) with the flow from left to right. The leading edge of the oscillating plate is visible near the center of the picture: a) oscillating plate on the right is moving upward and b) oscillating plate is moving downward.

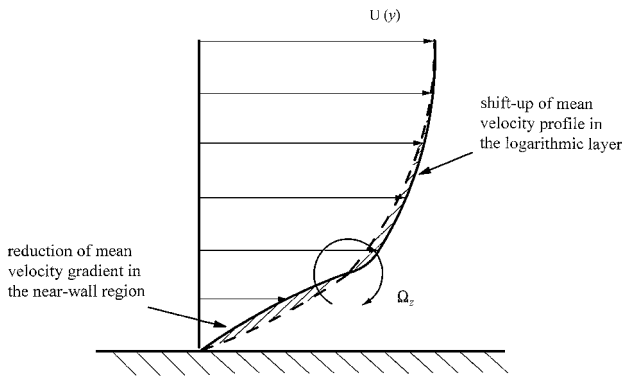


**Fig. 11** Conceptual model for a turbulent boundary layer over an oscillating wall, showing a spanwise vorticity  $\Omega_z$  created by the periodic Stokes layer.

move downstream in a sinuous form as the test plate oscillates in a spanwise direction. Figure 10a shows the near-wall boundary-layer structure over the oscillating plate as it moves upward, where the longitudinal vortices are twisted into the spanwise direction being realigned into the direction of an arrow. When the oscillating plate moves downward, the longitudinal vortices are twisted into an opposite direction as shown in Fig. 10b. The twisting action on the near-wall turbulence structure is caused by the periodic Stokes layer over the oscillating wall, which tilts the vorticity vector into the spanwise direction. The primary effect of the realignment of longitudinal vortices over the oscillating wall is to reduce the streamwise

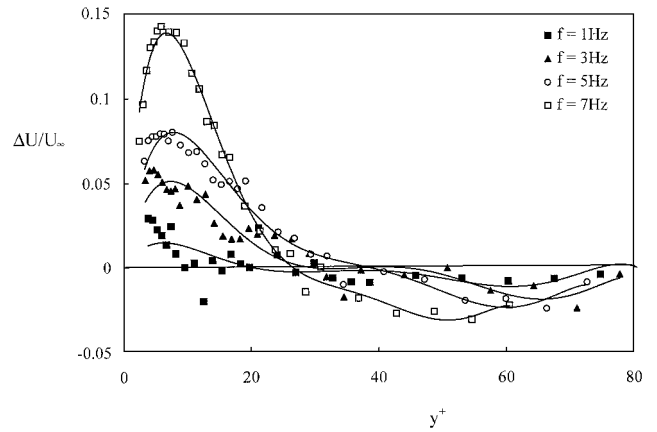


**Fig. 12** Velocity reductions  $\Delta u$  in the boundary-layer profiles 10 mm downstream from the trailing edge of the oscillating plate for different frequencies of wall oscillation ( $\Delta z = 70$  mm).

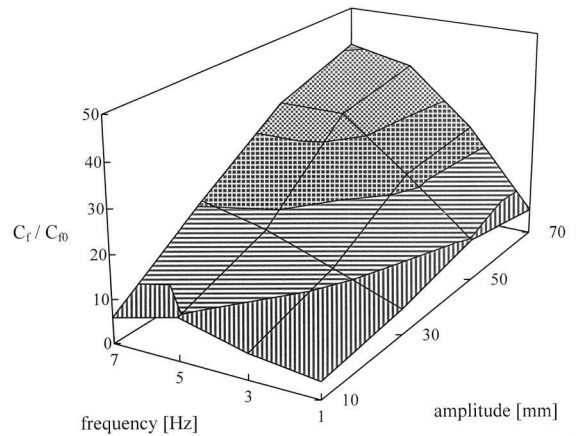


**Fig. 13** Turbulent skin-friction reduction due to spanwise-wall oscillation 10 mm downstream from the trailing edge of the oscillating plate as a function of frequency and amplitude of wall oscillation.

component of the vorticity near the wall. This is well supported by the DNS results,<sup>22</sup> indicating that the intensity of streamwise vorticity fluctuations is nearly halved across the entire thickness of the boundary layer as the wall oscillates in a spanwise direction. As a consequence, the near-wall burst<sup>15</sup> activity is weakened, leading to a reduction in turbulent skin-friction drag as observed in the present experiment. Here, the near-wall bursts are associated with the downdraft of high-momentum fluid toward the wall as a result of induction by the pairs of longitudinal vortices, which are the main source of turbulent energy production in the near-wall region of the boundary layer. Note that the tilting of the longitudinal vortices will only affect the streamwise component of vorticity because the spanwise realignment of the vortices takes place in alternate directions with the wall oscillation.

In general, the amount of skin-friction reduction is a function not only of the oscillation frequency but also of other parameters such as the oscillation amplitude as well as the Reynolds number of the Stokes layer introduced by the wall oscillation. Because the Reynolds number of the Stokes layer is well below the critical Reynolds number<sup>28–30</sup> in the present investigation, it is believed that the main parameters governing the turbulent boundary layer with spanwise-wall oscillation are the frequency and amplitude of wall oscillation. Figure 13 shows the amount of drag reduction measured at 10 mm ( $x^+ = 70$ ) downstream from the trailing edge of the oscillating plate, showing that the amount of drag reduction is indeed a function of both the frequency and the amplitude of wall oscillation. When the amount of drag reduction is plotted against the nondimensional wall speed  $\Delta z \cdot \omega / 2u^*$  (Fig. 14), all of the data seem to collapse on a single curve, confirming that the wall speed is indeed the key parameter of this flow problem. The maximum drag reduction by spanwise-wall oscillation could be obtained, therefore,

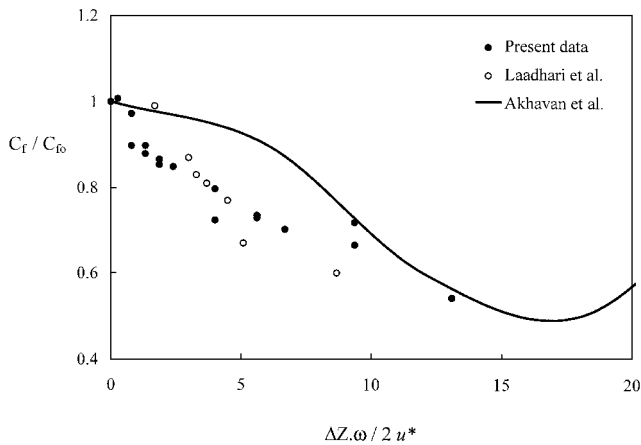


Fig. 14 Turbulent skin-friction reduction due to spanwise-wall oscillation as a function of nondimensional wall velocity.

by setting the nondimensional wall speed at an optimum value. The present results show that the turbulent skin-friction drag can be reduced with an increase in the wall speed of spanwise oscillation, but the saturation point does not seem to have been reached within the range of the present experimental parameters.

It has been known to the aeronautical community that the Reynolds stress of the three-dimensional turbulent boundary layer over a swept wing of an aircraft is less than that of the two-dimensional boundary layer.<sup>31–36</sup> Here, the turbulent boundary layer over the wing surface undergoes a spanwise pressure force due to the longitudinal pressure gradient developing from the swept leading edge of the wing. As a result, the boundary layer will be deflected toward the tip of the wing, forming a three-dimensional boundary layer. The turbulence models available at the present time cannot predict this anomaly very well, partly because the mechanism for the reduction of the Reynolds stress in the three-dimensional boundary layer is not well understood. The results of the present investigation seem to suggest that the spanwise-wall oscillation is effectively creating an unsteady three-dimensional boundary layer over the wall surface, thereby reducing the production of turbulent kinetic energy leading to a reduction in skin-friction drag. It has been suggested that the skin-friction reduction over the swept wing may be caused by a modification of the quasistreamwise vortices in the near-wall region by the spanwise shear of the three-dimensional boundary layer.<sup>35</sup> However, the modification of a near-wall turbulence structure by the spanwise shear of a steady, three-dimensional boundary layer is rather subtle,<sup>32</sup> possibly because the realignment angle of the longitudinal vortices by the spanwise shear over a swept wing is not very large. On the other hand, the spanwise-wall oscillation seems to be a very effective means of realigning the longitudinal vortices, where the drag reductions as much as 45% can be obtained by maintaining the three-dimensionality of the boundary-layer flow over an oscillating wall.

## Conclusions

A wind-tunnel study of the turbulent boundary layer with a spanwise-wall oscillation was carried out, where skin-friction reductions of as much as 45% were observed when the oscillation frequency and amplitude were adjusted to give an optimum speed of wall oscillation. With the logarithmic velocity profiles of the boundary layer shifted upward and the turbulence intensities reduced by the spanwise-wall oscillation, the present results convincingly confirmed the basic conclusions of the recent DNSs. It was also shown that the skewness and kurtosis of the velocity fluctuations are increased within the near-wall region, agreeing very well with the boundary-layer profiles of the DNS results with a wall oscillation.

It is believed that the mechanism of drag reduction by a spanwise-wall oscillation strongly relates to the spanwise vorticity generated by the periodic Stokes layer, which reduces the mean velocity gradient of the boundary layer within the viscous sublayer. The longitudinal vortices in the near-wall region are also realigned into the spanwise direction, reducing the intensity of streamwise vor-

ticity fluctuations across the boundary layer. As a result, the near-wall burst activity, which is associated with the downwash of high-momentum fluid near the wall, is weakened, leading to a reduction in turbulent skin-friction drag.

It seems that the effectiveness of turbulent drag reduction by the spanwise-wall oscillation can be improved with an increase in the twist angle of the vorticity vector, which is proportional to the ratio of the spanwise-wall velocity to the freestream velocity of the boundary layer. Indeed, it was demonstrated that the turbulent skin-friction drag is reduced with an increase in the wall speed of oscillation, which seems to be a key parameter in optimizing the turbulent drag reduction by spanwise-wall oscillation.

## Acknowledgments

The work was supported by Engineering and Physical Sciences Research Council Research Grants GR/J06917 and GR/K27780.

## References

- Liepmann, H. W., and Narasimha, R. (eds.), *Turbulence Management and Relaminarisation*, Springer-Verlag, Berlin, 1988, pp. 1–524.
- Bushnell, D. M., and McGinley, C. B., “Turbulent Control in Wall Flows,” *Annual Review of Fluid Mechanics*, Vol. 21, 1989, pp. 1–20.
- Bushnell, D. M., and Hefner, J. N. (eds.), *Viscous Drag Reduction in Boundary Layers*, Vol. 123, Progress in Astronautics and Aeronautics, AIAA, Washington, DC, 1990, pp. 1–509.
- Choi, K.-S. (ed.), *Recent Developments in Turbulence Management*, Kluwer, Dordrecht, The Netherlands, 1991, pp. 1–327.
- Choi, K.-S., Prasad, K. K., and Truong, T. V. (eds.), *Emerging Techniques in Drag Reduction*, Mechanical Engineering Publications, London, 1996, pp. 1–335.
- Kline, S. J., Reynolds, W. C., Schraub, F. A., and Runstadler, P. W., “The Structure of Turbulent Boundary Layers,” *Journal of Fluid Mechanics*, Vol. 30, 1967, pp. 741–773.
- Brown, G. L., and Roshko, A., “On Density Effects and Large Structure in Turbulent Mixing Layers,” *Journal of Fluid Mechanics*, Vol. 64, 1974, pp. 775–816.
- Townsend, A. A., *The Structure of Turbulent Shear Flow*, 2nd ed., Cambridge Univ. Press, Cambridge, England, UK, 1976, pp. 1–412.
- Head, M. R., and Bandyopadhyay, P., “New Aspects of Turbulent Boundary Layer Structure,” *Journal of Fluid Mechanics*, Vol. 107, 1981, pp. 297–338.
- Kravchenko, A. G., Choi, H., and Moin, P., “On the Relationship of Near-Wall Streamwise Vortices to Wall Skin Friction in Turbulent Boundary Layers,” *Physics of Fluids*, Vol. A5, No. 12, 1993, pp. 3307–3309.
- Choi, H., Moin, P., and Kim, J., “Active Turbulence Control for Drag Reduction in Wall-Bounded Flows,” *Journal of Fluid Mechanics*, Vol. 262, 1994, pp. 75–110.
- Orlandi, P., and Jimenez, J., “On the Generation of Turbulent Wall Friction,” *Physics of Fluids*, Vol. A6, No. 2, 1994, pp. 634–641.
- Choi, K.-S., “Turbulent Drag Reduction Strategies,” *Emerging Techniques in Drag Reduction*, edited by K.-S. Choi, K. K. Prasad, and T. V. Truong, Mechanical Engineering Publications, London, 1996, pp. 77–98.
- Bechert, D. W., and Bartenwerfer, M., “The Viscous Flow on Surfaces with Longitudinal Ribs,” *Journal of Fluid Mechanics*, Vol. 206, 1989, pp. 105–129.
- Choi, K.-S., “Near-Wall Structure of Turbulent Boundary Layer with Riblets,” *Journal of Fluid Mechanics*, Vol. 208, 1989, pp. 417–458.
- Walsh, M. J., “Riblets,” *Viscous Drag Reduction in Boundary Layers*, edited by D. M. Bushnell and J. N. Hefner, Vol. 123, Progress in Astronautics and Aeronautics, AIAA, Washington, DC, 1990, pp. 203–261.
- Coustols, E., “Riblets: Main Known and Unknown Features,” *Emerging Techniques in Drag Reduction*, edited by K.-S. Choi, K. K. Prasad, and T. V. Truong, Mechanical Engineering Publications, London, 1996, pp. 3–43.
- Bruse, M., Bechert, D. M., van der Hoeven, J. G. T., Hage, W., and Hoppe, G., “Experiments with Conventional and with Novel Adjustable Drag-Reducing Surfaces,” *Near-Wall Turbulent Flows*, edited by R. M. C. So, C. G. Speziale, and B. E. Launder, Elsevier, Amsterdam, 1993, pp. 719–738.
- Anders, J. B., “Outer-Layer Manipulators for Turbulent Drag Reduction,” *Viscous Drag Reduction in Boundary Layers*, edited by D. M. Bushnell and J. N. Hefner, Vol. 123, Progress in Astronautics and Aeronautics, AIAA, Washington, DC, 1990, pp. 263–284.
- Savill, A. M., “Drag Reduction by Passive Devices—A Review of Some Recent Development,” *Structure of Turbulence and Drag Reduction*, edited by A. Gyr, Springer-Verlag, Berlin, 1990, pp. 429–465.
- Jung, W. J., Mangiavacchi, N., and Akhavan, R., “Suppression of Turbulence in Wall-Bounded Flows by High Frequency Spanwise Oscillations,” *Physics of Fluids*, Vol. A4, No. 8, 1992, pp. 1605–1607.

- <sup>22</sup>Baron, A., and Quadrio, M., "Turbulent Drag Reduction by Spanwise Wall Oscillations," *Applied Scientific Research*, Vol. 55, 1996, pp. 311–326.
- <sup>23</sup>Laadhari, F., Skandaji, L., and Morel, R., "Turbulence Reduction in a Boundary Layer by a Local Spanwise Oscillating Surface," *Physics of Fluids*, Vol. A6, No. 10, 1994, pp. 3218–3220.
- <sup>24</sup>Dean, R. B., "A Single Formula for the Complete Velocity Profile in a Turbulent Boundary Layer," *Journal of Fluids Engineering*, Vol. 98, No. 4, 1976, pp. 723–727.
- <sup>25</sup>Durst, F., Jovanovic, J., and Sender, J., "LDA Measurements in the Near-Wall Region of a Turbulent Pipe Flow," *Journal of Fluid Mechanics*, Vol. 295, 1995, pp. 305–335.
- <sup>26</sup>Pal, S., Deutsch, S., and Merkle, C. L., "A Comparison of Shear Stress Fluctuation Statistics Between Microbubble Modified and Polymer Modified Turbulent Boundary Layers," *Physics of Fluids*, Vol. A1, No. 8, 1989, pp. 1360–1362.
- <sup>27</sup>Sherman, F. S., *Viscous Flow*, McGraw-Hill, New York, 1990, pp. 137–140.
- <sup>28</sup>Sarpkaya, T., "Coherent Structures in Oscillatory Boundary Layers," *Journal of Fluid Mechanics*, Vol. 253, 1993, pp. 105–140.
- <sup>29</sup>Akhavan, R., Kamm, R. D., and Shapiro, A. H., "An Investigation of Transition to Turbulence in Bounded Oscillatory Stokes Flows, Part 1. Experiments," *Journal of Fluid Mechanics*, Vol. 225, 1991, pp. 395–422.
- <sup>30</sup>Akhavan, R., Kamm, R. D., and Shapiro, A. H., "An Investigation of Transition to Turbulence in Bounded Oscillatory Stokes Flows, Part 2. Numerical Simulations," *Journal of Fluid Mechanics*, Vol. 225, 1991, pp. 423–444.
- <sup>31</sup>Elsenaar, A., and Boelsma, S. H., "Measurements of the Reynolds Stress Tensor in a Three-Dimensional Turbulent Boundary Layer Under Infinite Swept Wing Conditions," National Aerospace Lab. (NLR), TR 74095U, Delft, The Netherlands, 1974.
- <sup>32</sup>Bradshaw, P., and Pontikos, N. S., "Measurements in a Turbulent Boundary Layer on an Infinite Swept Wing," *Journal of Fluid Mechanics*, Vol. 159, 1985, pp. 105–130.
- <sup>33</sup>Baskaran, V., Pontikos, Y. G., and Bradshaw, P., "Experimental Investigation of Three-Dimensional Turbulent Boundary Layers on Infinite Swept Curved Wings," *Journal of Fluid Mechanics*, Vol. 211, 1990, pp. 95–122.
- <sup>34</sup>Flack, K. A., and Johnston, J. P., "Experimental Study of a Detaching Three-Dimensional Turbulent Boundary Layer," *Near-Wall Turbulent Flows*, edited by R. M. C. So, C. G. Speziale, and B. E. Launder, Elsevier, Amsterdam, 1993, pp. 977–986.
- <sup>35</sup>Schwarz, W. R., and Bradshaw, P., "Turbulence Structural Changes for a Three-Dimensional Turbulent Boundary Layer in a 30° Bend," *Journal of Fluid Mechanics*, Vol. 272, 1994, pp. 183–209.
- <sup>36</sup>Coleman, G. N., Kim, J., and Le, A.-T., "A Numerical Study of Three-Dimensional Wall-Bounded Flows," *International Journal of Heat and Fluid Flow*, Vol. 17, No. 3, 1996, pp. 333–342.

P. R. Bandyopadhyay  
Associate Editor